Int. J. Engng Sci. Vol. 28, No. 12, pp. 1347–1358, 1990
Printed in Great Britain.
0020-7225/90 $3.00 + 0.00

AN APPROXIMATE ANALYSIS OF STEADY STATE AXISYMMETRIC DEFORMATIONS OF VISCOPLASTIC TARGETS

R. C. BATRA and XINGJU CHEN

Department of Mechanical and Aerospace Engineering and Engineering Mechanics, University of Missouri-Rolla, Rolla, MO 65401-0249, U.S.A.

Abstract—Steady state axisymmetric deformations of a viscoplastic target being penetrated by a rigid cylindrical penetrator with a hemispherical nose are analyzed. The presumed kinematically admissible velocity field satisfies all of the boundary conditions on the target/penetrator interface, and also the balance of mass. The unknown parameters appearing in the admissible velocity field are found by minimizing the error in satisfying the balance of linear momentum. The solution so obtained is found to be very close to the finite element solution of the problem. An advantage of the present technique is the enormous savings in the computational effort and resources required to analyze the problem.

1. INTRODUCTION

In recent years, emphasis has been placed on kinetic energy penetrators, which for terminal ballistic purposes may be considered as long metal rods traveling at high speeds. For impact velocities in the range of 2–10 km/s, incompressible hydrodynamic flow equations can be used to describe adequately the impact and penetration phenomena, because large stresses occurring in hypervelocity impact permit one to neglect the rigidity and compressibility of the striking bodies. Models, which require the use of the Bernoulli equation or its modification to describe this hypervelocity impact, have been proposed by Birkhoff *et al.* [1] and Pack and Evans [2]. At ordnance velocities (0.5–2 km/s), the material strength becomes an important parameter. Allen and Rogers [3] modified the Pack and Evans [2] flow model by representing the strength as a resistive pressure. This idea was taken further by Alekseevskii [4] and Tate [5, 6], who considered separate resistive pressures for the penetrator and the target. These resistive pressures are empirically determined quantities, and the predicted results depend strongly upon the assumed values of these pressures. As described by Wright [7] in his survey article on long rod penetrators, Tate's model is difficult to use for quantitative purposes, because the strength parameters depend upon the velocity of impact and the particular combination of materials involved. Wright and Frank [8] in their reexamination of Tate's theory, have derived expressions for the resistive pressures in terms of mass densities, yield strengths of the penetrator and target material, and penetrator speed.

The paper by Backman and Goldsmith [9] is an authoritative review of the open literature on ballistic penetration, containing 278 reference citations from the 1800s to 1977. They describe different physical mechanisms involved in the penetration and perforation processes, and also discuss a number of engineering models. Jonas and Zukas [10] reviewed various analytical methods for the study of kinetic energy projectile–armor interaction at ordnance velocities and placed particular emphasis on three-dimensional numerical simulation of perforation. Anderson and Bodner [11] have recently reviewed engineering models for penetration and some of the major advances in hydrocode modeling of penetration problems. Two books [13, 14], published during the past few years, include extensive discussions of the engineering models, experimental techniques and analytical modeling of ballistic perforation.

Awerbuch [15], Awerbuch and Bodner [16], Ravid and Bodner [17], and Ravid *et al.* [18] have developed models to analyze the normal perforation of metallic plates by projectiles. The penetration process is presumed to occur in several interconnected stages, with plug formation and ejection being the principal mechanism of plate perforation. They presumed a kinematically admissible flow field and found the unknown parameters by minimizing the plastic dissipation. They characterized the procedure as being a modification of the upper bound theorem of plasticity to include dynamic effects. These authors have included the dependence of the yield stress upon the strain rate and studied a purely mechanical problem.

Jones *et al.* [19] have modified the one-dimensional eroding-rod penetration theory of Tate by accounting for the mass transfer from the rigid end of the rod into the plastic region, and the mushroom strain at the deforming end of the rod. Their results suggest that the latter factor has a substantial effect on calculated penetrations. Woodward [20] has proposed a one-dimensional model of penetration which regards both penetrator and target as mushrooming cylinders and the target flow stress is increased to account for the lateral constraint. A finite difference formulation is used for both target and projectile to divide them into a series of elements. The projectile elements which enter the target are subjected to lateral constraint and a shear stress if their diameter is sufficient to touch the edges of the hole. Forrestal *et al.* [21] have used the cavity expansion model to predict the penetration depths for relatively rigid projectiles striking deformable semi-infinite targets.

The one-dimensional theories ignore the lateral motion, plastic flow and the detailed dynamic effects. In an attempt to understand better the approximations made in simpler theories of penetration, Batra and Wright [22] studied the problem of a rigid cylindrical rod with a hemispherical nose penetrating into a rigid/perfectly plastic target. The target deformations, as seen by an observer moving with the penetrator nose tip, were presumed to be steady. Subsequently Batra and his coworkers [23–28] studied the effect of nose shape, strain hardening, strain-rate hardening and thermal softening characteristics of the target material and also analyzed the steady state axisymmetric deformations of a rod striking a rigid cavity. Guided by the results given in [22, 23] we presume a kinematically admissible velocity field to analyze the steady state axisymmetric deformations of a viscoplastic target being penetrated by a rigid hemispherical nosed cylindrical rod. The approximate solution obtained herein compares favorably with the finite element solution and requires less than one-hundredth of the computational resources in terms of the CPU time and the storage requirements.

2. FORMULATION OF THE PROBLEM

We use the Eulerian description of motion and a cylindrical coordinate system with origin at the center of the hemispherical nose and moving with it at a uniform speed v_0 to describe the deformations of the target. The positive z-axis is taken to point into the target. We work in terms of non-dimensional variables indicated below by a superimposed bar.

$$\bar{\boldsymbol{\sigma}} = \boldsymbol{\sigma}/\sigma_0, \qquad \bar{p} = p/\sigma_0, \qquad \alpha = \rho_0 v_0^2/\sigma_0,$$
$$\bar{\mathbf{v}} = \mathbf{v}/v_0, \qquad \bar{r} = r/r_0, \qquad \bar{z} = z/r_0, \tag{1}$$

where $\boldsymbol{\sigma}$ is the Cauchy stress tensor, p the hydrostatic pressure not determined by the deformation history since the deformations are assumed to be isochoric, $\mathbf{v} = (v_r, v_z)$ is the velocity of a material particle, the pair (r, z) describe the current position of a material particle, r_0 is the radius of the undeformed cylindrical portion of the rod, ρ_0 equals the mass density of a target material and σ_0 is the yield stress of the target material in a quasistatic simple compression test. The non-dimensional parameter α equals the magnitude of the inertia forces relative to the flow stress of the material.

Hereafter, we drop the superimposed bars. Equations governing the deformations of the target are

$$\operatorname{div} \mathbf{v} = 0, \tag{2.1}$$

$$\operatorname{div} \boldsymbol{\sigma} = \alpha(\mathbf{v} \cdot \operatorname{grad})\mathbf{v}, \tag{2.2}$$

$$\boldsymbol{\sigma} = -p\mathbf{1} + \frac{(1 + bI)^m}{\sqrt{3}I}\mathbf{D}, \tag{2.3}$$

$$2\mathbf{D} = \operatorname{grad} \mathbf{v} + (\operatorname{grad} \mathbf{v})^T, \tag{2.4}$$

$$2I^2 = \operatorname{tr}(\mathbf{D}^2). \tag{2.5}$$

Equations (2.1) and (2.2) express, respectively, the balance of mass and the balance of linear momentum. Equation (2.3) is the constitutive relation for the rigid/viscoplastic target material.

It may be written as

$$S_e \equiv \left(\frac{1}{2}\operatorname{tr}(\mathbf{s}^2)\right)^{1/2} = (1+bI)^m/\sqrt{3}, \tag{3.1}$$

$$\mathbf{s} = \boldsymbol{\sigma} + p\mathbf{1}. \tag{3.2}$$

The kinetic equation (3.1) is of a specific overstress form—roughly similar to that proposed by Cowper–Symonds–Bodner and generalized by Perzyna. The parameters b and m describe the strain-rate hardening characteristics of the material. $\mathbf{D}$, given by equation (2.4), is the strain-rate tensor and I is its second invariant. Equation (2.1) and the one obtained by substituting (2.3) into (2.2) are the nonlinear partial differential equations to be solved for $\mathbf{v}$ and p under the prescribed boundary conditions.

At the target/penetrator interface, we impose the boundary conditions

$$\mathbf{t}\cdot(\boldsymbol{\sigma}\mathbf{n}) = 0, \tag{4.1}$$

$$\mathbf{v}\cdot\mathbf{n} = 0, \tag{4.2}$$

where $\mathbf{n}$ and $\mathbf{t}$ are, respectively, a unit normal and a unit tangent to the surface. The boundary condition (4.2) ensures that there is no interpenetration of the target material into the penetrator, and the boundary condition (4.1) states that the target/penetrator interface is smooth. This seems reasonable because a thin layer of material at the interface either melts or is severely degraded by adiabatic shear. At points far away from the penetrator,

$$|\mathbf{v}+\mathbf{e}| \to 0 \quad \text{as} \quad |\mathbf{x}| = (r^2+z^2)^{1/2} \to \infty, \qquad z > -\infty, \tag{5.1}$$

$$|\boldsymbol{\sigma}\mathbf{n}| \to 0 \quad \text{as} \quad z \to -\infty, \tag{5.2}$$

where $\mathbf{e}$ is a unit vector in the positive z-direction. The boundary condition (5.1) states that target particles far away from the penetrator appear to be moving with a uniform speed with respect to it. Equation (5.2) states that far to the rear the traction field vanishes. Note that the governing equations (2.1)–(2.3) are nonlinear in $\mathbf{v}$ and their solution, if there exists one, will depend on the rates at which quantities in (5) decay to zero.

3. AN APPROXIMATE SOLUTION

Guided by the finite element solutions [22, 23] of the corresponding problem, we divide the deforming target region shown in Fig. 1 into two subregions: region I and region II. We assume that in region I the target material extrudes rearward as a uniform block. Thus, the velocity of

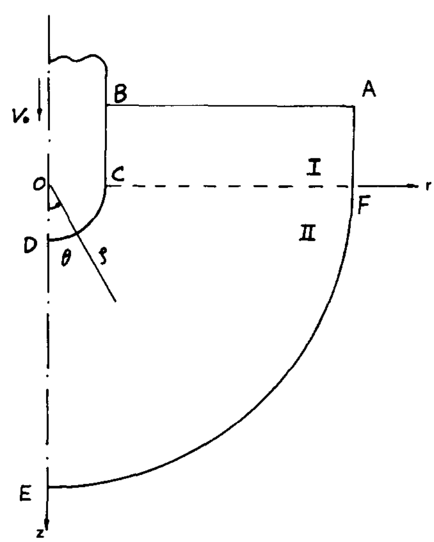

Fig. 1. The problem studied.

material particles in this region is along the axis of the rod. We note that a similar assumption was made by Ravid and Bodner [17] in their analysis of the perforation of thick plates. In order to describe the velocity field in region II, we introduce a new coordinate system (ρ, θ) where

$$\rho = (r^2 + z^2)^{1/2}, \tag{6.1}$$

$$\theta = \tan^{-1}(r/z). \tag{6.2}$$

Thus

$$v_\theta = v_r \cos\theta - v_z \sin\theta, \tag{7.1}$$

$$v_\rho = v_r \sin\theta + v_z \cos\theta. \tag{7.2}$$

Equation (2.1), and the boundary conditions (4.2) and (5.1) take the form

$$\frac{\partial v_\rho}{\partial \rho} + \frac{1}{\rho}\frac{\partial v_\theta}{\partial \theta} + \frac{2v_\rho}{\rho} + \frac{v_\theta \cos\theta}{\rho \sin\theta} = 0, \tag{8}$$

$$v_\rho = 0 \quad \text{on CD and } v_\theta = 0 \text{ on DE}, \tag{9.1}$$

$$v_z \to -1, \qquad v_r = 0 \quad \text{as} \quad \rho \to \infty. \tag{9.2}$$

We also need to ensure that on CF

$$\mathbf{v}_{\mathrm{I}} = \mathbf{v}_{\mathrm{II}}, \tag{10.1}$$

and

$$(\boldsymbol{\sigma}\mathbf{n})_{\mathrm{I}} = (\boldsymbol{\sigma}\mathbf{n})_{\mathrm{II}}. \tag{10.2}$$

If the boundary EF is far enough from the noise tip D, then condition (9.2) is a reasonable approximation to (5.1). The condition (9.1) on DE follows from the assumption that the deformations are axisymmetric.

A velocity field that satisfies equation (8), boundary conditions (9.1) and (9.2), and the continuity condition (10.1) and exhibits characteristics similar to that found by the finite element solution is given below. In region II,

$$v_\theta = \left(1 - \frac{1}{\rho^{n+1}} + \frac{1}{\rho^n}\right)\sin\theta + \sum_{m,k} C_{mk}\rho^m \sin^k 2\theta, \tag{11.1}$$

$$v_\rho = \left[\left(\frac{1}{\rho^2} - 1\right)\cos\theta - \frac{2}{1-n}\left(\frac{1}{\rho^2} - \frac{1}{\rho^{n+1}}\right)\cos\theta + \frac{2}{2-n}\left(\frac{1}{\rho^2} - \frac{1}{\rho^n}\right)\cos\theta\right] - \sum_{m,k}\frac{C_{mk}}{m+2}\left(\frac{1}{\rho^2} - \rho^m\right)\sin^{k-1} 2\theta((2k+1)\cos 2\theta + 1), \tag{11.2}$$

and in region I

$$v_z = -\left(1 - \frac{1}{r^{n+1}} + \frac{1}{r^n}\right), \qquad v_r = 0. \tag{12}$$

In equation (11), the constants n and C_{mk} are yet to be determined. The natural boundary conditions (4.1) and (5.1), and that on the axis of symmetry DE can be written as

$$\sigma_{\rho\theta} = 0 \quad \text{on DC}, \tag{13.1}$$

$$|\boldsymbol{\sigma}\mathbf{n}| \to 0 \quad \text{as } \rho \to \infty, \tag{13.2}$$

$$\sigma_{rz} = 0 \quad \text{on DE}. \tag{13.3}$$

Recalling the constitutive relation (2.3), we see that boundary conditions (13.1) and (13.3) are equivalent to

$$\frac{\partial v_\theta}{\partial \rho} + \frac{1}{\rho}\frac{\partial v_\rho}{\partial \theta} - \frac{v_\theta}{\rho} = 0 \qquad \text{when } \rho = 1 \text{ or } \theta = 0. \tag{14}$$

This is satisfied if we choose

$$m \leqslant -3, \qquad k \geqslant 3, \qquad \sum_m C_{mk}(m-1) = 0, \qquad k = 3, 4, \ldots. \tag{15}$$

The satisfaction of the boundary condition (13.2) requires that

$$|p| \to 0, \quad \text{as} \quad \rho \to \infty. \tag{16}$$

In order to determine the hydrostatic pressure p, we use the balance of linear momentum (2.2). Substitution from (11), (7) and (2.3) into (2.2) gives

$$\frac{\partial p}{\partial r}=f(r,z), \tag{17.1}$$

$$\frac{\partial p}{\partial z}=g(r,z), \tag{17.2}$$

where f and g are known functions of r and z. Their expressions are quite long and are omitted. Since it is hard to choose n and C_{mk} such that the integrability condition

$$\frac{\partial f}{\partial z}-\frac{\partial g}{\partial r}=0 \tag{18}$$

is satisfied, we find n and C_{mk} by ensuring that the functional

$$J(n,C_{mk})=\int_{\Omega}\left(\frac{\partial f}{\partial z}-\frac{\partial g}{\partial r}\right)^2 \mathrm{d}\Omega \tag{19}$$

takes on the minimum value. Knowing n and C_{mk}, the pressure is found by integrating equation (17) and the constant of integration is determined by setting $p=0$ at $\rho=1$, $\theta=90°$. This condition is also taken from the finite element solution of the problem. The computed pressure field does satisfy (16). However, no attempt was made to achieve the rate of decay of p equal to that obtained in a finite element solution of the problem.

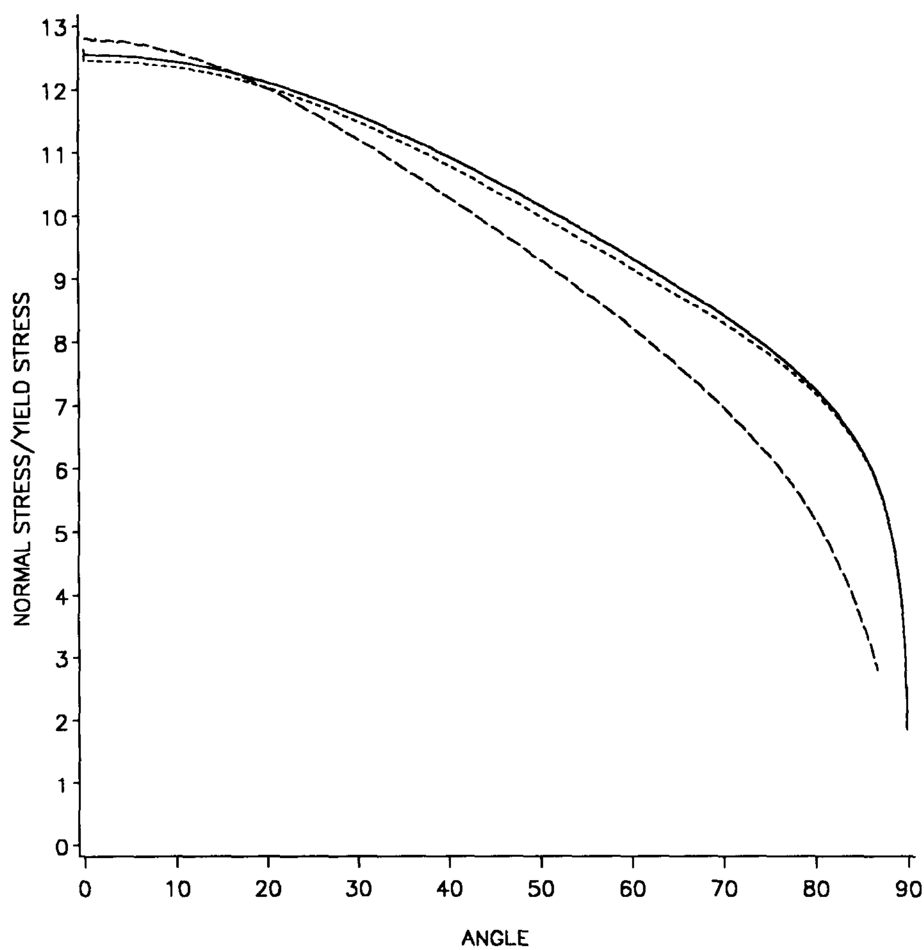

Fig. 2. Distribution of the normal traction on the penetrator nose. —— One term solution; ----- three terms solution; – – – FEM solution.

Having determined σ in region II we can use the balance of linear momentum, boundary conditions (10.2) and (5.2) to compute the stress field in the region I. However, the computation of this stress field is not necessary in order to compute various quantities of practical interest.

4. DISCUSSION OF RESULTS

In order to compare the solution obtained with the present method with that computed by the finite element method, we set $b = 10^4$ s, $m = 0.03$ and $\alpha = \rho_0 v_0^2/\sigma_0 = 6.15$. Whenever different values of b, m and α are used, these are stated in the figure captions. Figure 2 depicts the distribution of the normal traction on the penetrator nose. The solution computed with the leading term in equation (11) differs very little from that found by also including the next two terms in the series. These two solutions match well with the finite element solution for $0 \leqslant \theta \leqslant 25°$. For $\theta > 25°$, the presently computed solution differs noticeably from the finite element solution. Because of very little difference between the leading term solution and the three terms solution, it was felt that the consideration of the additional terms in the series will not result in any significant improvement in the solution. The variation of the second invariant I of the strain-rate tensor $\mathbf{D}$ along the axial line, plotted in Fig. 3, reveals that the results obtained with the present method are very close to the finite element solution of the problem. In this case, the three terms solution and the one term solution overlapped each other. However, the computed values of σ_{zz} on the axial line, shown in Fig. 4, do not agree that well

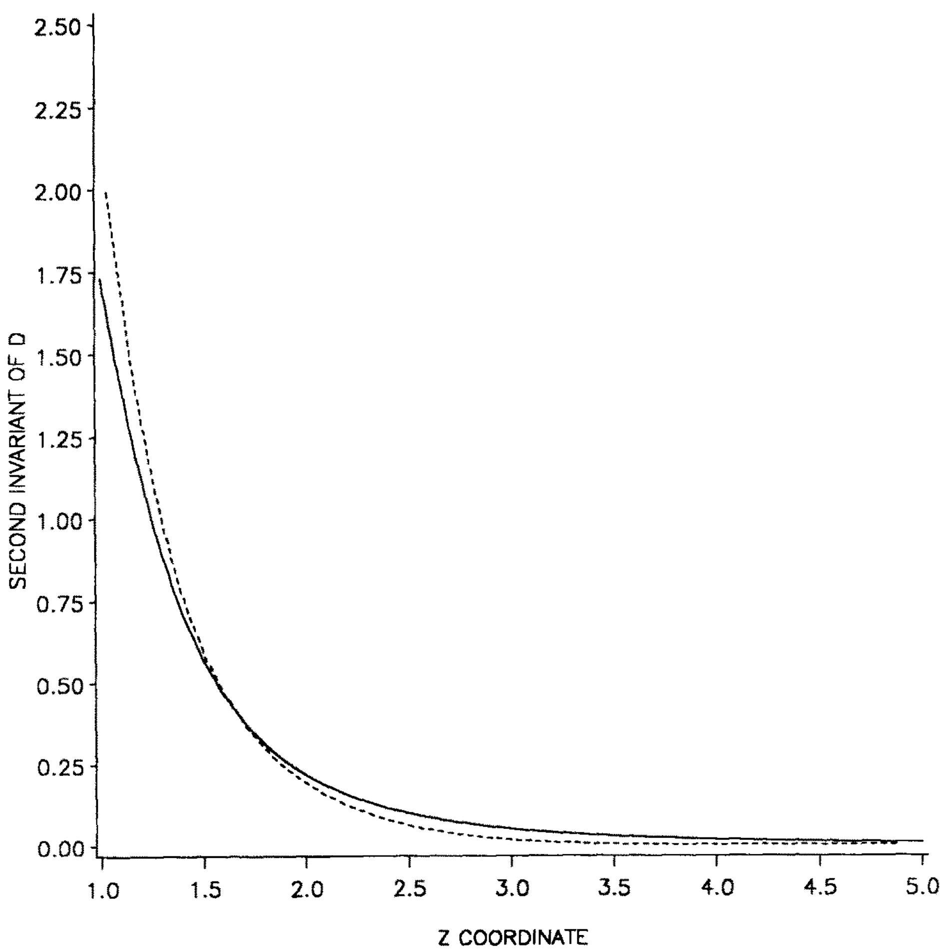

Fig. 3. Variation of the second invariant I of the strain-rate tensor on the axial line. —— Present solution; - - - - - finite element solution.

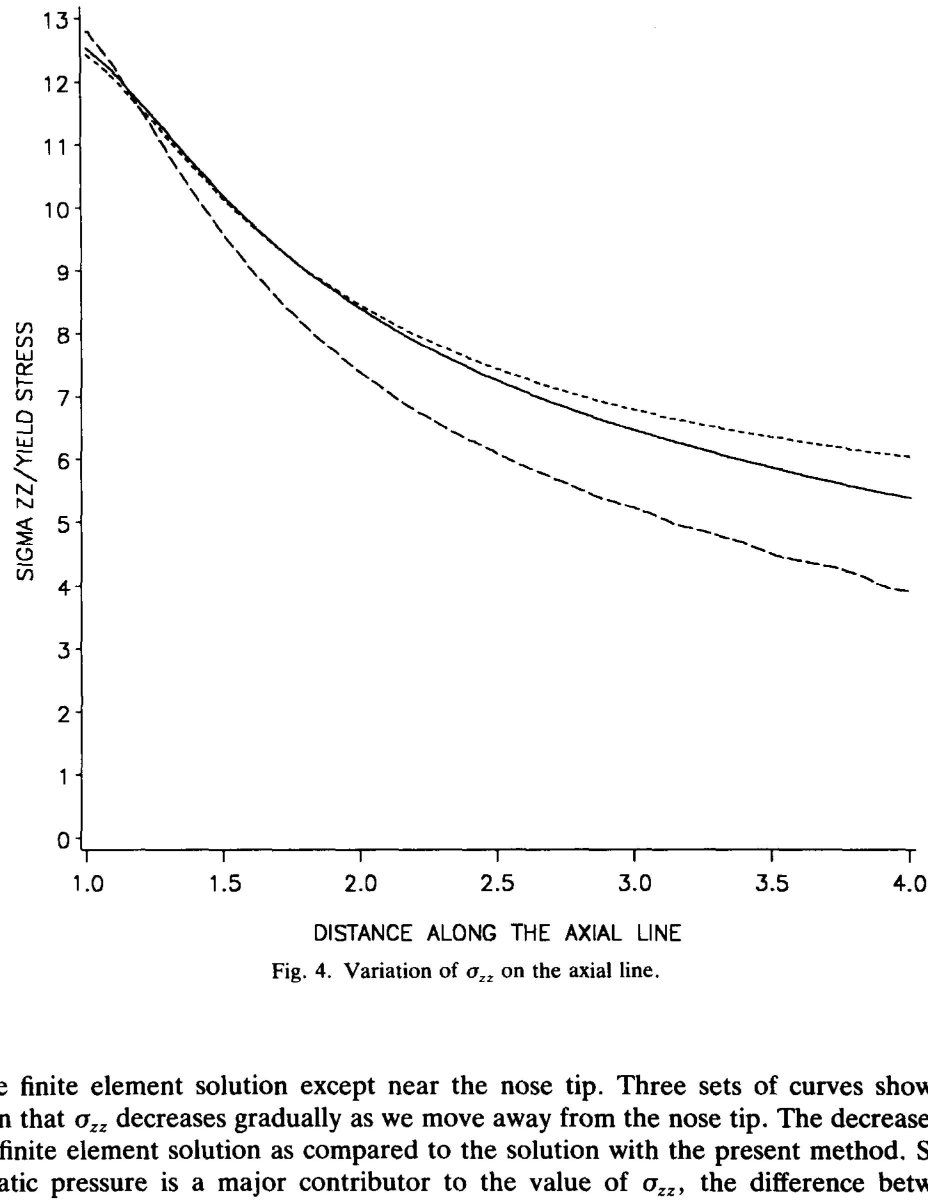

Fig. 4. Variation of σ_{zz} on the axial line.

with the finite element solution except near the nose tip. Three sets of curves show similar trends in that σ_{zz} decreases gradually as we move away from the nose tip. The decrease is more for the finite element solution as compared to the solution with the present method. Since the hydrostatic pressure is a major contributor to the value of σ_{zz}, the difference between the present solution and the finite element solution can be attributed to the different rates of decay of p. We note that many results of practical importance computed with the present method, as outlined below, are close to those obtained from the finite element solution.

On the axial line, the Bernoulli equation, as modified by Tate [5, 6] is

$$\frac{1}{2}\rho_0 v_s^2 + R_t = -\sigma_{zz}(1, 0) \tag{20}$$

where R_t accounts for the strength of the target material. Having computed σ_{zz} and knowing $\rho_0 v_s^2$, we can find R_t. The value of R_t thus computed equals 9.43 σ_0 with the present method and 9.63 σ_0 with the finite element method. From Fig. 3, we see that at the nose tip $\mathrm{I} = 1.75$. Since $v_0/r_0 = 1.48 \times 10^5\ \mathrm{s}^{-1}$, therefore, at the nose tip

$$\sigma_D = \sigma_0(1 + 10^4(1.75 \times 1.48 \times 10^5))^{0.03} = 1.916\sigma_0 \tag{21}$$

where σ_D is the value of the flow stress for the target material at a strain-rate of $2.59 \times 10^5\ \mathrm{s}^{-1}$. Thus $R_t = 4.92\sigma_D$ for the presently computed solution. The non-dimensional axial resisting

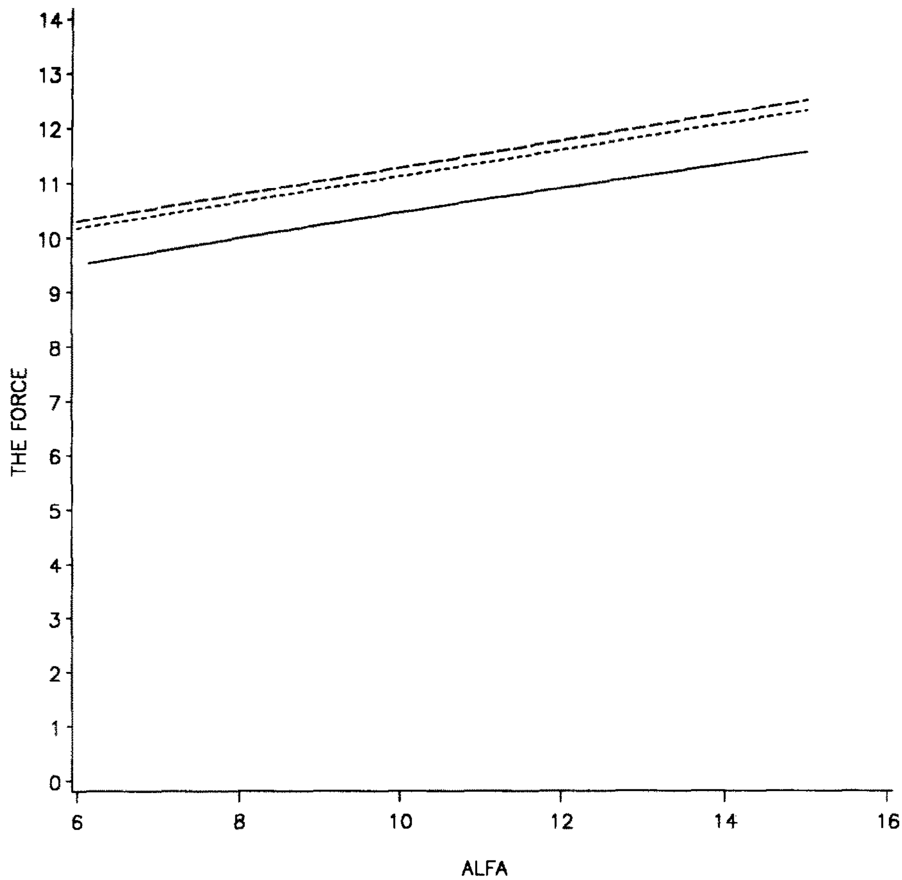

Fig. 5. Dependence of the axial resisting force upon α. —— Finite element solution; ----- one term solution; – – – three terms solution.

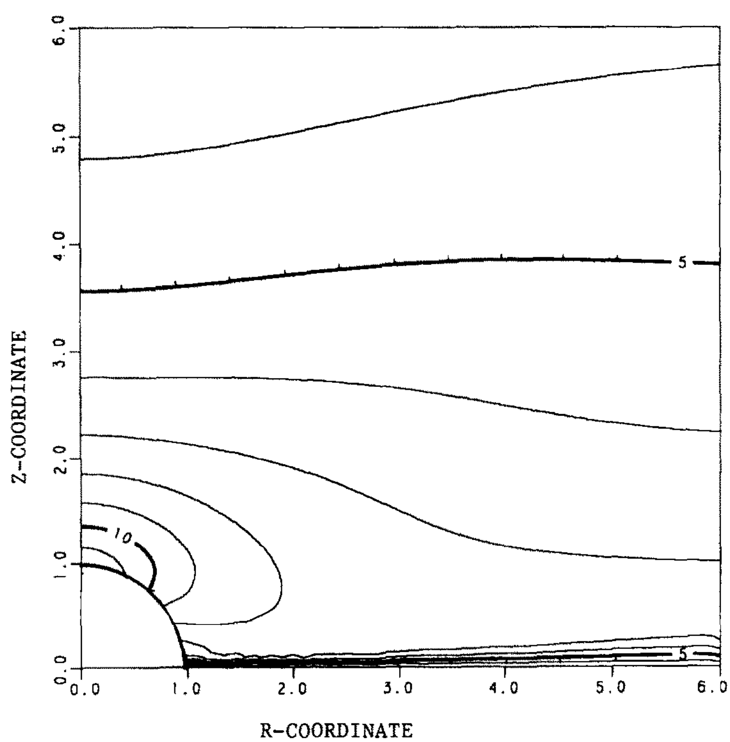

Fig. 6. Contours of the hydrostatic pressure in the deforming target region.

force F experienced by the penetrator is given by

$$F = \int_0^{\pi/2} (\mathbf{n} \cdot \boldsymbol{\sigma}\mathbf{n}) \sin 2\theta \, d\theta. \tag{22}$$

The dimensional values of the resisting force equal $\pi r_0^2 \sigma_0 F$. Figure 5, which is a plot of F vs α, shows that the dependence of F upon α is rather weak. Equations of straight lines fitted by the least squares method to the computed data are

$$F = 8.575 + 0.197\alpha, \text{ FEM solution,} \tag{23.1}$$

$$F = 8.717 + 0.243\alpha, \text{ Present 3 terms solution.} \tag{23.2}$$

Thus the two methods yield virtually identical values of F. The weak dependence of F upon α indicates why the choice of the constant target resistance in the simple theory of Tate [5, 6] gives good qualitative results.

The contours of the hydrostatic pressure p plotted in Fig. 6 indicate that the pressure near the nose tip is very high and it drops off rather slowly as we move away from the nose tip. It is thus obvious that the hydrostatic pressure near the penetrator nose makes a significant contribution to the normal traction acting on the nose tip and hence to the axial resisting force experienced by the penetrator. In Fig. 7, we have plotted the distribution of the normal traction on the penetrator nose for different values of α. As expected, the normal traction at a point on the penetrator nose increases with α. In the finite element solution [22] of the problem, the normal traction at $\theta = 45°$ was unaffected by the value of α. It seems that this was

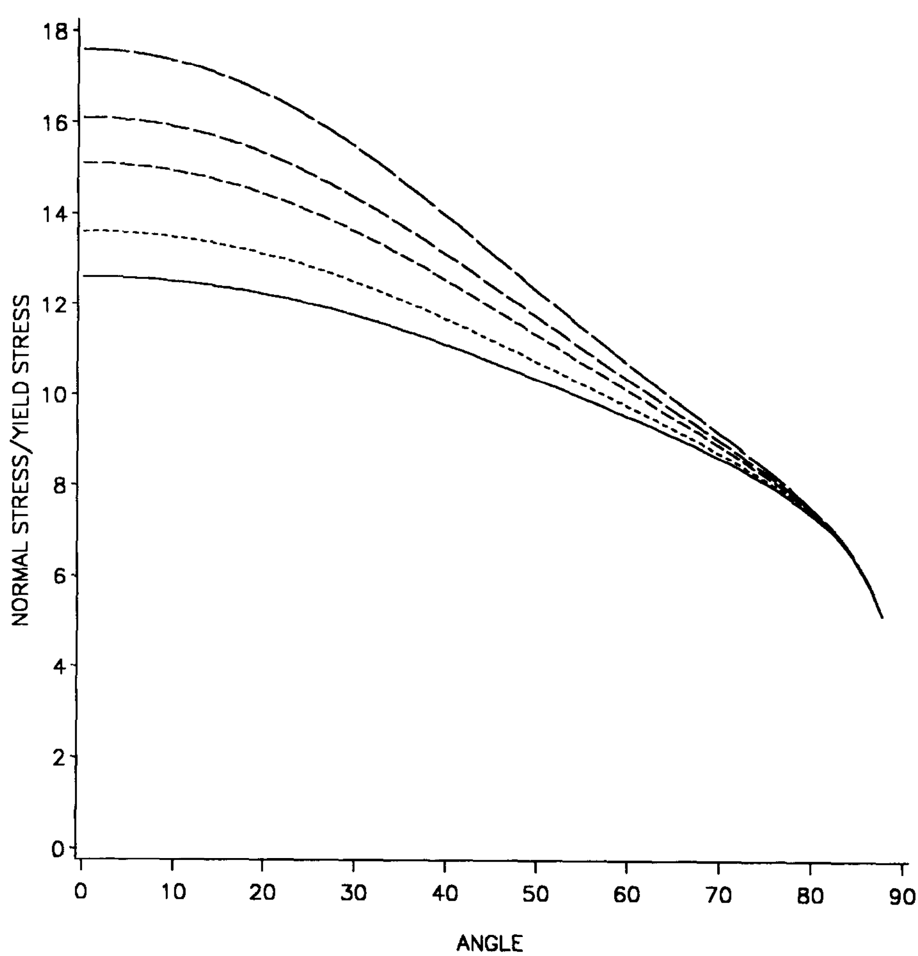

Fig. 7. Dependence of the normal traction on the penetrator nose upon α. —— $\alpha = 5$; - - - - - $\alpha = 7$; - - - $\alpha = 10$; — — — $\alpha = 12$, ——— ——— $\alpha = 15$. $m = 0.05$.

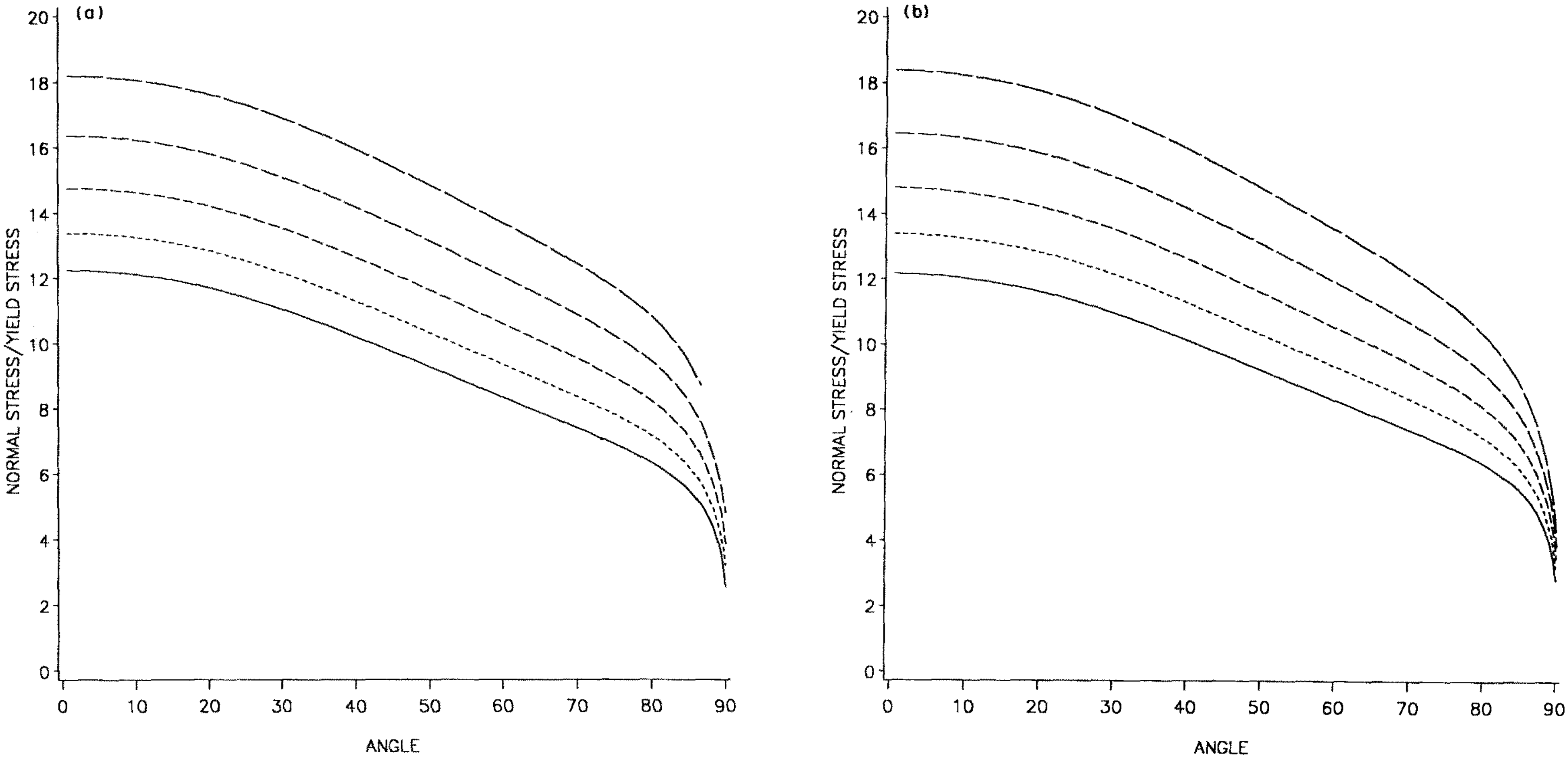

Fig. 8. Dependence of the normal stress acting on the penetrator nose upon the values of b and m. (a) —— $b = 10^2$; - - - - - $b = 10^4$; – – – $b = 10^6$; —— —— $b = 10^8$; ——— ——— $b = 10^{10}$; $\alpha = 8$, $m = 0.03$. (b) —— $m = 0.01$; - - - - - $m = 0.03$; – – – $m = 0.05$; —— —— $m = 0.07$; ——— ——— $m = 0.09$; $\alpha = 8$.

due to the coarse mesh used. Since at $\theta = 0°$, the normal traction on the penetrator nose equals $(-\sigma_{zz})$, and the deviatoric part of the stress equals 0.667 for the rigid/perfectly plastic target material and a little bit more for the viscoplastic target material, the hydrostatic pressure at the nose tip increases significantly with the increase in the value of α.

Figures 8(a) and (b) depict respectively the dependence of the normal stress on the penetrator nose upon the values of b and m that characterize the viscoplastic response of the target material. It is obvious that the normal stress on the penetrator nose and hence the axial resisting force acting on the penetrator depend strongly upon the values of b and m. As the value of either b or m is increased, the normal stress at a point on the penetrator nose, except near the periphery of the nose, increases sharply. Recall that at $\theta = 90°$, p is set equal to 0 during the solution of the problem. The dependence of the axial resisting force upon m and b is depicted in Fig. 9. These plots show that F depends strongly upon b and m as was also found to be the case in the finite element solution of the problem.

We note that Forrestal *et al.* [29] have given the depth of penetration of hemispherical nosed steel rods penetrating into aluminum targets impacted at different speeds. From their data, it is hard to estimate the resisting force experienced by the rod during the steady state portion of the penetration process. Also the assumption in our work that the contact at target/penetrator interface is smooth should be modified to account for the frictional forces acting on the interface. Since the assumed kinematically admissible velocity field gives zero tangential tractions at the contact surface, the consideration of frictional forces there necessitates that we modify the velocity field.

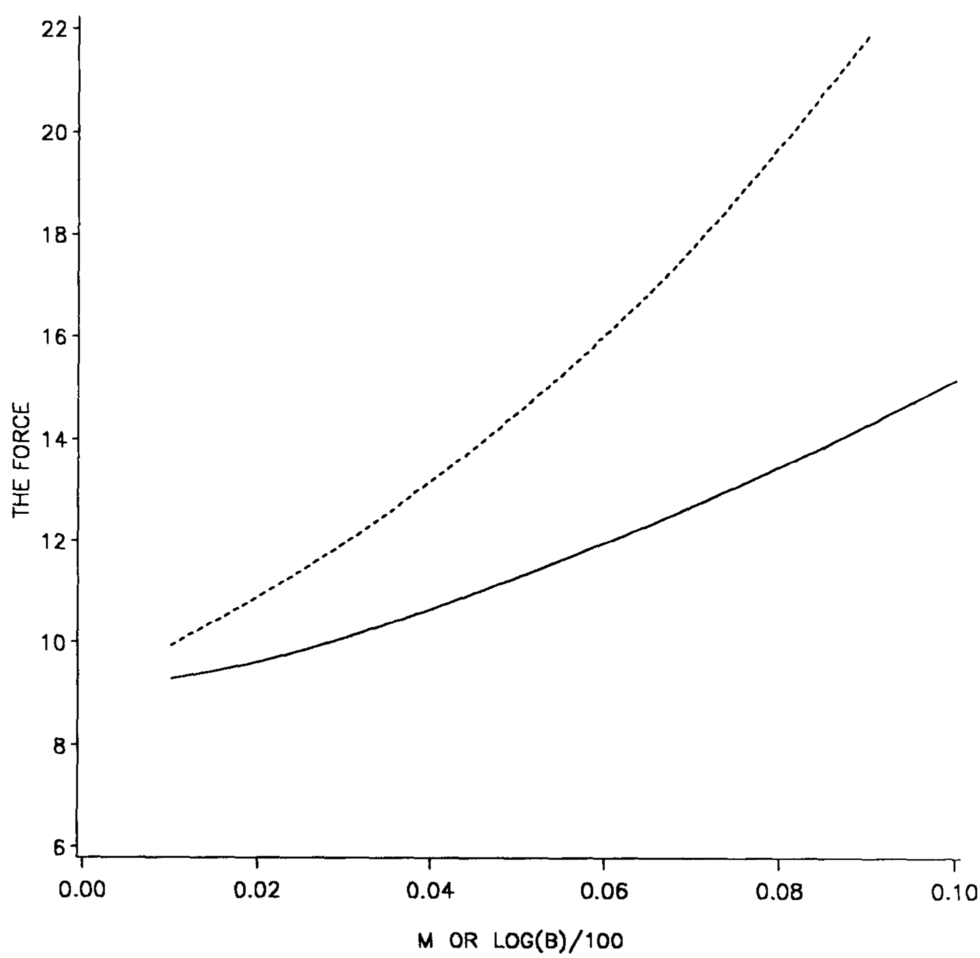

Fig. 9. Dependence of the axial resisting force experienced by the penetrator upon the values of b and m. —— b; - - - - m; $\alpha = 8.0$.

5. CONCLUSIONS

A simple approximate solution to the problem of analyzing axisymmetric steady state deformations of a rigid-viscoplastic target being penetrated by a long rigid cylindrical rod with a hemispherical nose is presented. A kinematically admissible velocity field that satisfies the balance of mass, all of the essential boundary conditions, and traction boundary conditions on the axis of symmetry and the target/penetrator interface is proposed. The various parameters in the presumed velocity field are found by minimizing the error in the satisfaction of the balance of linear momentum. The computed results reveal that the leading term in the proposed velocity field gives a good solution that is reasonably close to the finite element solution [22, 23]. The axial resisting force experienced by the penetrator is found to depend weakly upon the square of the penetrator speed but strongly upon the strain-rate hardening exponent for the target material. The value of the resisting force term suggested by Tate [5, 6] in the modified Bernoulli equation is found to be 9.43 σ_0 or $4.92\sigma_D$ where σ_D is the dynamic flow stress for the target material at a value of the strain-rate equal to that prevailing at the stagnation point.

Acknowledgement–This work was supported by the U.S. Army Research Office Contract DAAL03-89-K-0050 to the University of Missouri-Rolla.

REFERENCES

[1] G. BIRKHOFF, D. P. MCDOUGALL, E. M. PUGH and G. TAYLOR, *Proc. Phys. Soc. Lond.* **57**, 147 (1945).
[2] D. C. PACK and W. M. EVANS, *Proc. Phys. Soc. Lond.* **B64**, 298 (1951).
[3] W. A. ALLEN and J. W. ROGERS, *J. Franklin Inst.* **272**, 275 (1961).
[4] V. P. ALEKSEEVSKII, *Combust. Explo. Shock Waves* **2**, 63 (1966).
[5] A. TATE, *J. Mech. Phys. Solids* **15**, 387 (1967).
[6] A. TATE, *J. Mech. Phys. Solids* **17**, 141 (1969).
[7] T. W. WRIGHT, *Lecture Notes in Engineering*, Vol. 3, *Computational Aspects of Penetration Mechanics* (Edited by J. CHANDRA and J. FLAHERTY). Springer, New York (1984).
[8] T. W. WRIGHT and K. FRANK, BRL Technical Report No. 2957 (1988).
[9] M. E. BACKMAN and W. GOLDSMITH, *Int. J. Engng Sci.* **16**, 1 (1978).
[10] G. H. JONAS and J. A. ZUKAS, *Int. J. Engng Sci.* **16**, 879 (1978).
[11] C. E. ANDERSON and S. R. BODNER, *Int. J. Impact Engng* **7**, 9 (1988).
[12] E. W. BILLINGTON and A. TATE, *The Physics of Deformation and Flow*. McGraw–Hill, New York (1981).
[13] J. A. ZUKAS, T. NICHOLAS, H. F. SWIFT, L. B. GRESZCZUK and D. R. CURRAN, *Impact Dynamics*. Wiley, New York (1982).
[14] M. MACAULEY, *Introduction to Impact Engineering*. Chapman & Hall, London (1987).
[15] J. AWERBUCH, Technion–Israel Institute of Technology, MED Report No. 28 (1970).
[16] J. AWERBUCH and S. R. BODNER, *Int. J. Solids Struct.* **10**, 671 (1974).
[17] M. RAVID and S. R. BODNER, *Int. J. Engng Sci.* **21**, 577 (1983).
[18] M. RAVID, S. R. BODNER and I. HOLCMAN, *Int. J. Engng Sci.* **25**, 473 (1987).
[19] S. E. JONES, P. O. GILLIS and J. C. FOSTER, *J. Mech. Phys. Solids* **35**, 121 (1987).
[20] R. L. WOODWARD, *Int. J. Mech. Sci.* **24**, 73 (1982).
[21] M. J. FORRESTAL, K. OKAJIMA and V. K. LUK, *Proc. 1st Joint SES/ASME-AMD Conf.*, Univ. of California at Berkeley (1988).
[22] R. C. BATRA and T. W. WRIGHT, *Int. J. Engng Sci.* **24**, 41 (1986).
[23] R. C. BATRA, *Int. J. Engng Sci.* **25**, 1131 (1987).
[24] R. C. BATRA, *Comp. Mechs.* **3**, 1 (1988).
[25] R. C. BATRA and PEI-RONG LIN, *Int. J. Engng Sci.* **26**, 183 (1988).
[26] R. C. BATRA and PEI-RONG LIN, *Int. J. Impact Engng* **8**, 99 (1989).
[27] R. C. BATRA and T. GOBINATH, *Int. J. Engng Sci.* **26**, 741 (1988).
[28] PEI-RONG LIN and R. C. BATRA, *Int. J. Engng Sci.* **27**, 1155 (1989).
[29] M. J. FORRESTAL, N. S. BRAR and V. K. LUK, *Computational Techniques for Contact, Impact, Penetration and Perforation of Solids* (Edited by L. E. SCHWER, N. J. SALAMON and W. K. LIU), pp. 215–222. ASME Press, New York (1989).

(Revision received and accepted 21 June 1990)